

OPEN ACCESS

# ZnTe Amorphous Semiconductor Nanowires Array Electrodeposited into Polycarbonate Membrane Thin Films

To cite this article: T Ohgai *et al* 2013 *J. Phys.: Conf. Ser.* **417** 012005

View the [article online](#) for updates and enhancements.

## You may also like

- [Surface modification of a-plane sapphire substrates and its effect on crystal orientation of ZnTe layer](#)  
Taizo Nakasu, Wei-Che Sun and Masakazu Kobayashi
- [DFT insights into the selective NH<sub>3</sub> sensing mechanism of two dimensional ZnTe monolayer](#)  
Xiao Chang, Xiaofang Li and Qingzhong Xue
- [Synthesis and characterization of pure and Sb/Sn doped ZnTe for solar cell application](#)  
Neha Pandey, Brijesh Kumar and D K Dwivedi



**ECS**  
The  
Electrochemical  
Society  
Advancing solid state &  
electrochemical science & technology

**DISCOVER**  
how sustainability  
intersects with  
electrochemistry & solid  
state science research

# ZnTe Amorphous Semiconductor Nanowires Array Electrodeposited into Polycarbonate Membrane Thin Films

T. Ohgai<sup>1</sup>, T. Ikeda<sup>2</sup> and J. Ohta<sup>3</sup>

<sup>1</sup>Division of Chemistry and Materials Science, Nagasaki University, 1-14 Bunkyo-machi, Nagasaki 852-8521, JAPAN

<sup>2</sup>Graduate School of Science & Technology, Nagasaki University, 1-14 Bunkyo-machi, Nagasaki 852-8521, JAPAN

<sup>3</sup>Department of Materials Science and Engineering, Nagasaki University, 1-14 Bunkyo-machi, Nagasaki 852-8521, JAPAN

E-mail: ohgai@nagasaki-u.ac.jp

**Abstract.** ZnTe amorphous semiconductor nanowires array was electrodeposited into the nanochannels of ion-track etched polycarbonate membrane thin films from acidic aqueous solution at 313 K. ZnTe electrodeposits with Zn-rich composition was obtained over the wide range of cathode potential from -0.8 V to -1.1 V and the growth rate of ZnTe amorphous nanowires was around 3 nm·sec<sup>-1</sup> at the cathode potential of -0.8 V. Cylindrical shape of the nanowires was precisely transferred from the nanochannels and the aspect ratio reached up to ca. 40. ZnTe amorphous phase electrodeposited at 313 K was crystallized by annealing at 683 K and the band gap energy of ZnTe crystalline phase reached up to ca. 2.13 eV.

## 1. Introduction

II-VI compound semiconductors (CdSe, CdTe, ZnSe, ZnTe, *etc.* [1, 2]) with wide band gap energy can be applied to the opto-electronic devices. Among of the II-VI compound semiconductors, ZnTe can be applied to green light emission diodes and photovoltaic solar cells because the band gap energy is 2.26 eV, which corresponds to around 550 nm. ZnTe thin films can be prepared using several techniques such as, thermal evaporation [3], sputtering [4], chemical vapor deposition [5] and electrodeposition from aqueous [6-9] or non-aqueous [10-13] solution. By the way, one-dimensional semiconductor nanowires with a large aspect ratio have received much attention due to their shape anisotropy and extremely large surface area [14, 15]. Nanowires can be fabricated by electrochemically depositing metallic atoms into a nano-well template with numerous nanochannels such as anodized aluminum oxide films or polycarbonate membrane films [16-18]. T. Gandhi *et al.* [19] and Y. Liu *et al.* [20] reported that ZnTe nanowires or nanoparticles can be electrodeposited into an anodized titanium oxide nanotubes array. However, for the opto-electronic device application, it is quite difficult to obtain the uniform structure of electrodeposited ZnTe nanowires array using a conductive titanium oxide template. In this paper, ZnTe amorphous semiconductor nanowires array was synthesized into the nanochannels of non-conductive ion-track etched polycarbonate membrane thin films to obtain a novel semiconductor device with extremely large surface area. Crystallization process and optical properties of the electrodeposited ZnTe were also investigated.

## 2. Experimental Procedures

**Figure 1** shows experimental apparatus for electrodeposition of ZnTe thin films and nanowires. Bath composition and electrolysis condition are also shown in this figure. Aqueous electrolytic solutions were synthesized from  $\text{ZnSO}_4 \cdot 7\text{H}_2\text{O}$  (0.1 M),  $\text{TeO}_2$  (0.002 M),  $\text{Na}_2\text{SO}_4$  (0.5 M),  $\text{H}_3\text{Cit}$  (citrate acid: 0.05 M) and  $\text{Na}_3\text{Cit} \cdot 2\text{H}_2\text{O}$  (sodium citrate: 0.05 M). The solution pH was adjusted to 4.0 by adding sulfuric acid and sodium hydroxide and the solution temperature was kept to 313K. Glass sheets coated with ITO were used as a cathode for growing ZnTe thin films, while ion track-etched polycarbonate membrane films were used as a template for growing ZnTe nanowires. Optimum deposition potential for growing ZnTe was determined by a cathodic polarization curve measured over the wide range of potential window. ZnTe were electrodeposited potention-statically keeping the cathode potential to -0.8 V. Crystal phase, structure and chemical composition of electrodeposited ZnTe was investigated by using XRD and EDX. Band gap energy of ZnTe was estimated by using UV-VIS absorption spectroscopy.

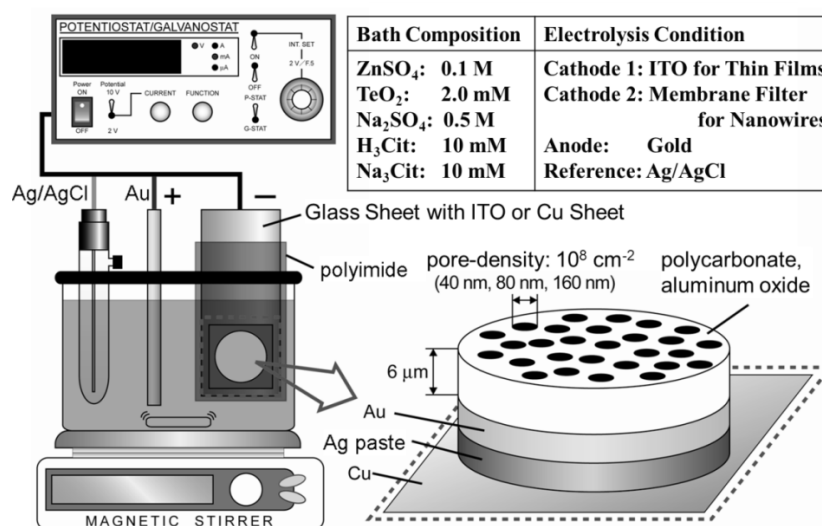
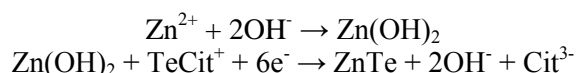


**Figure 1.** Experimental apparatus for electrodeposition of ZnTe thin films and nanowires (Bath composition and electrolysis condition are also shown in this figure).

## 3. Results and Discussion

### 3-1. Electrodeposition process of ZnTe nanowires

Cathodic polarization curve for electrodeposition of ZnTe from an aqueous solution containing  $\text{Zn}^{2+}$  and  $\text{TeCit}^+$  ions is shown in **Fig.2**. At the potential of ca. -0.2 V,  $\text{TeCit}^+$  ions began to be reduced. With increasing the current up to  $10^{-2} \text{ A/m}^2$ , the potential polarized to around -0.4 V and  $\text{H}^+$  ions began to deposit. With increase in the current over  $10 \text{ A/m}^2$ , the potential polarized from -0.4 V to -1.0 V. In this potential range, the pH in the vicinity of the cathode can increase up to around 6 due to the diffusion limit of  $\text{H}^+$  ions and  $\text{TeCit}^+$  ions, then  $\text{Zn(OH)}_2$  forms in the vicinity of cathode. Electrodeposition of ZnTe will proceed by Zn UPD due to the formation of  $\text{Zn(OH)}_2$  by the following reaction.



Zn-Te films deposited in the potential range from -0.8 V to -0.9 V mainly contained ZnTe phase with stoichiometric composition. Furthermore, with increase in the current more than  $50 \text{ A/m}^2$ , the potential polarized to less-noble than -1.0 V. In the potential range, massive metallic Zn began to deposit from  $\text{Zn(OH)}_2$ .

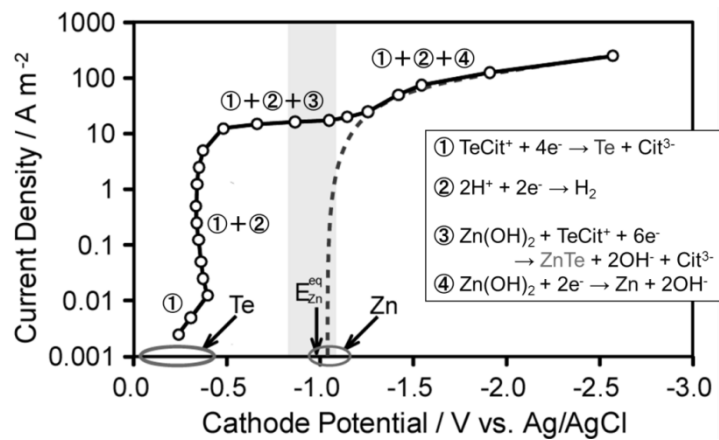


**Figure 2.** Cathodic polarization curve for electrodeposition of ZnTe from an aqueous solution containing  $\text{Zn}^{2+}$  and  $\text{TeCit}^+$  ions.

**Figure 3** shows the effect of cathode potential on Zn content in electrodeposits obtained from aqueous solutions containing  $\text{Zn}^{2+}$  and  $\text{TeCit}^+$  ions. In the cathode potential range less-nobler than -0.9 V, Zn content in electrodeposit was more than 60%. On the other hand, in the cathode potential range nobler than -0.8 V, Zn content in electrodeposit was close to 50%. T. Ishizaki *et al.* reported that the potential-pH diagram at pH4.7 of Zn-Te-Cit- $\text{H}_2\text{O}$  system and predicted that ZnTe can be electrodeposited over the wide range of cathode potential from -0.45 V to -1.1 V [21]. Therefore, in this study, ZnTe electrodeposits with Zn-rich composition could be obtained over the wide range of cathode potential from -0.8 V to -1.1 V.

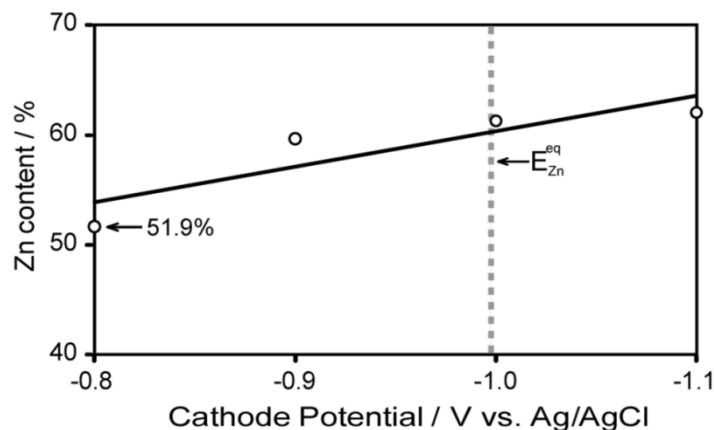


**Figure 3.** Effect of cathode potential on Zn content in electrodeposits obtained from aqueous solutions containing  $\text{Zn}^{2+}$  and  $\text{TeCit}^+$  ions.

**Figure 4** shows effect of cathode potential on the time-dependence of cathodic current during electrodeposition of ZnTe nanowires. To determine the growth rate of nanowires, the filling time of a nanochannel 6000 nm in length was estimated by monitoring the time-dependence of deposition current at each cathode potential as shown in **Fig.4**. When the nanochannels are filled and the nanowires reach the membrane surface, the current will increase drastically due to the formation of hemispherical caps. The growth rates were estimated by dividing channel length by channel-filling time. At -0.7 V, the filling time is around 3000 s and the deposition rate is estimated to be about  $2 \text{ nm s}^{-1}$ , while the filling time is close to 2000 s at -0.8 V and the deposition rate is estimated to be around  $3 \text{ nm s}^{-1}$ .

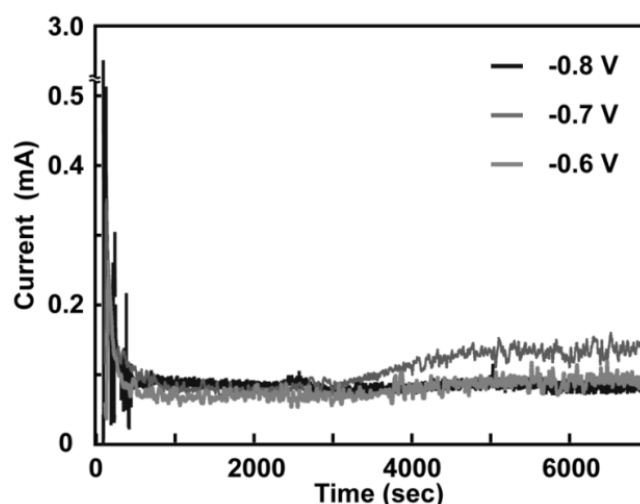


**Figure 4.** Effect of cathode potential on the time-dependence of cathodic current during electrodeposition of ZnTe nanowires.

SEM images of electrodeposited ZnTe nanowires separated from polycarbonate membrane filters with pore diameter 160nm are shown in **Fig.5**. The cylindrical shape was precisely transferred from the nanochannels to the nanowires and the aspect ratio reached up to ca. 40.

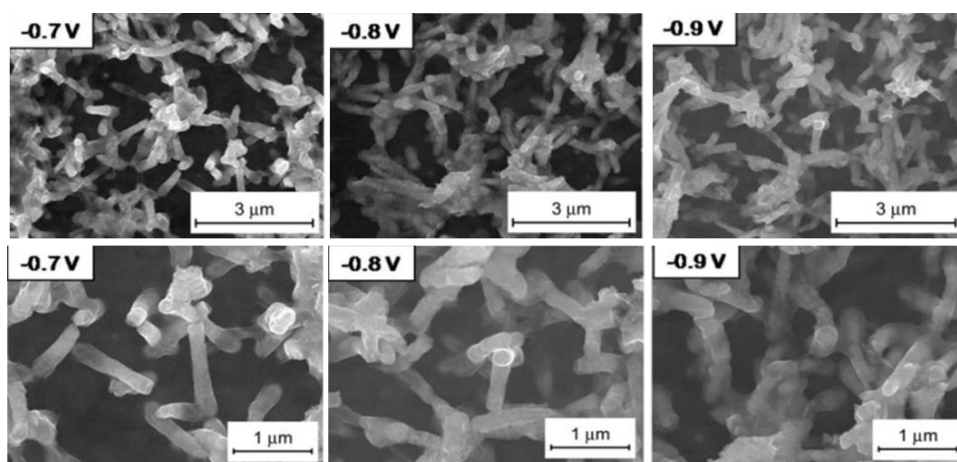


**Figure 5.** SEM images of ZnTe nanowires electrodeposited at -0.7 V, -0.8 V and -0.9 V. Nanowires were separated from polycarbonate membrane filters with pore diameter 160nm.

### 3-2. Crystallization process and optical properties of electrodeposited ZnTe

XRD patterns for as-deposited ZnTe films and annealed ZnTe films are shown in **Fig.6**. As-deposited ZnTe was composed from an amorphous phase, while the deposit was crystallized with annealing at 653 K for 5 hours and that contained binary phases of ZnTe and Te. On the other hand, the deposit with annealing at 683 K for 5 hours contained a single phase of ZnTe. A. B. Kashyout *et al.* reported that ZnTe electrodeposition from an aqueous solution containing  $\text{ZnCl}_2$ ,  $\text{TeO}_2$  and HCl [22]. They found that the electrodeposits annealed at 623 K composed from Te single phase, while the deposits annealed at 648 K and 673 K consist of ZnTe single phase. Melting points of Te and ZnTe are 718 K and 1563 K. Therefore, higher annealing temperature would be necessary to obtain ZnTe single phase.

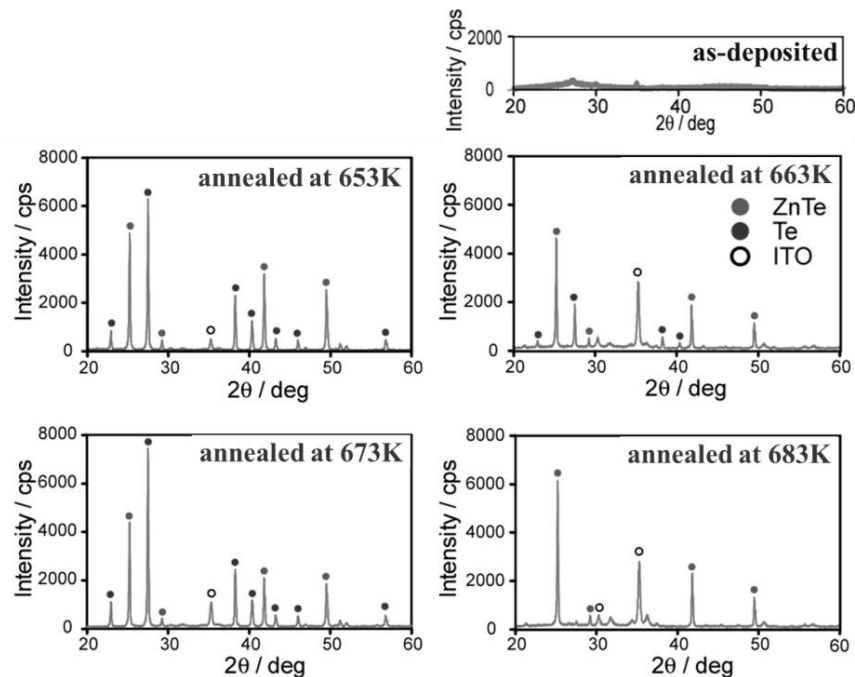


**Figure 6.** XRD patterns for as-deposited ZnTe, annealed at 653 K, 663 K, 673 K and 683 K.

UV-VIS absorption spectra and  $(\alpha h\nu)^2$  vs.  $h\nu$  plot for determining the band gap energy of electrodeposited ZnTe are shown in **Fig.7**. In the wave length range less than around 550nm, optical absorption behavior was observed in the deposit with a single phase of ZnTe. Therefore, the band gap energy of the deposit with ZnTe single phase was estimated to be around 2.13 eV. M. Neumann-Spallart *et al.* reported that ZnTe electrodeposition on TCO (F-doped  $\text{SnO}_2$  covered glass) from an aqueous solution containing  $\text{ZnSO}_4$ ,  $\text{TeO}_2$  and  $\text{K}_2\text{SO}_4$  [23]. They estimated that the band gap energy of electrodeposited ZnTe are around 2.15 eV which is quite close to our experimental data.

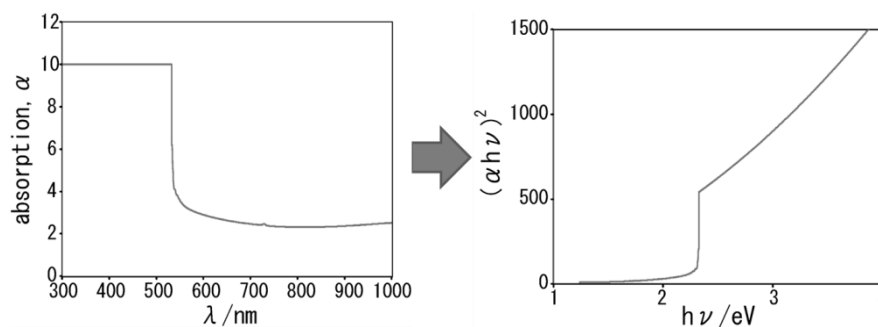


**Figure 7.** UV-VIS absorption spectra and  $(\alpha h\nu)^2$  vs.  $h\nu$  plot for determining the band gap energy of electrodeposited ZnTe.

#### 4. Conclusions

Optimum cathode potential for electrodeposition of ZnTe was determined to be -0.8 V and the growth rate of ZnTe nanowires was around  $3 \text{ nm} \cdot \text{sec}^{-1}$ . As-deposited ZnTe was composed from an amorphous phase, while the deposit was crystallized with annealing and band gap energy of the deposit with ZnTe single phase showed 2.13 eV.

## Acknowledgement

This work was supported in part by Japan Society for the Promotion of Science (Grant-in-aid for Scientific Research C : No. 21560748), The President's Discretionary Fund of Nagasaki University, JFE 21st Century Foundation and Kyushu Industrial Technology Center.

## References

- [1] Gu J, Tonomura K, Yoshikawa N, Sakaguchi T 1973 *J. Appl. Phys.* **44** 4692
- [2] Winnewisser C, Jepsen P U, Schall M, Schiyja V, Helm H 1997 *Appl. Phys. Lett.* **70** 3069
- [3] Pal U, Saha S, Chaudhuri A K, Rao V V, Banerjee H D 1989 *J. Phys. D: Appl. Phys.* **22** 965
- [4] Bellakhder H, Outzourhit A, Ameziane E L 2001 *Thin Solid Films* **382** 30
- [5] Wolf K, Stanzl H, Naumov A, Wagner H P, Kuhn W, Kahn B, Gebhardt W 1994 *J. Cryst. Growth* **138** 412
- [6] Bulent M. Basol, Vijay K. Kapur 1988 *Thin Solid Films* **165** 237
- [7] Bozzini B, Baker M A, Cavallotti P L, Cerri E, Lenardi C 2000 *Thin Solid Films* **361-362** 388
- [8] Bozzini B, Lenardi C, Lovergine N 2000 *Mater. Chem. Phys.* **66** 219
- [9] Bouroushian M, Kosanovic T, Karoussos D, Spyrellis N 2009 *Electrochem. Acta* **54** 2522
- [10] Chaure N B, Nair J P, Jayakrishnan R, Ganesan V, Pandey R K 1998 *Thin Solid Films* **324** 78
- [11] Lin M C, Chen P Y, Sun I W 2001 *J. Electrochem. Soc.* **148** C653
- [12] Heo P, Ichino R, Okido M 2006 *Electrochem. Acta* **51** 6325
- [13] Islam A B M O, Chaure N B, Wellings J, Tolan G, Dharmadasa I M 2009 *Mater. Character.* **60** 160
- [14] Ohgai T, Gravier L, Hoffer X, Ansermet J P 2005 *J. Appl. Electrochem.* **35** 479
- [15] Kim D J, Seol J K, Lee M R, Hyung J H, Kim G S, Ohgai T, Lee S K 2012 *Appl. Phys. Lett.* **100** 163703
- [16] Ohgai T, Enculescu I, Zet C, Westerberg L, Hjort K, Spohr R, Neumann R 2006 *J. Appl. Electrochem.* **36** 1157
- [17] Ohgai T, Hjort K, Spohr R, Neumann R 2008 *J. Appl. Electrochem.* **38** 713
- [18] Spohr R, Zet C, Bernd Fischer B E, Kiesewetter H, Apel P, Gunko I, Ohgai T, Westerberg L 2010 *Nucl. Inst. Meth. Phys. Res.* **B268** 676
- [19] Gandhi T, Raja K S, Misra M 2009 *Thin Solid Films* **517** 4527
- [20] Liu Y, Zhang X, Liu R, Yang R, Liu C, Cai Q 2011 *J. Solid State Chem.* **184** 684
- [21] Ishizaki T, Saito N, Takai O, Asakura S, Goto K, Fuwa A 2005 *Electrochem. Acta* **50** 3509
- [22] Kashyout A B, Arico A S, Antonucci P L, Mohamed F A, Antonucci V 1997 *Mater. Chem. Phys.* **51** 130
- [23] Neumann-Spallart M, Königstein C 1995 *Thin Solid Films* **265** 33